give similar results.[14] It is thus apparent that the binding energy–charge relationships are to be regarded primarily as useful correlations and not necessarily as absolute representations of physical reality. It is noteworthy, however, that in some very recent Hartree–Fock calculations[15] on various carbon ions, the Koopmans' theorem 1s binding energy increased by 0.56 hartree from the neutral atom to the unipositive ion. This is similar to the present results (Table VI) that from CH_4 to CHF_3 a 1s binding energy increase of 0.54 hartree occurs for an effective carbon atom charge change of 0.83 e.

Despite the difficulty of defining atomic charges, once a choice is made one can then obtain a "feel" for the relative charges of atoms in different environments, and thus gain useful insight into inner-shell binding energies and their relations to molecular structure.[6] Hopefully, the discussions here will encourage other researchers to consider these matters of dipole moments, atomic charges, and inner-shell energy levels in relation to one another.

Acknowledgments. The work of M. E. S. at Notre Dame is partially supported by a grant from the Petroleum Research Fund administered by the American Chemical Society, and that of L. C. A. at Princeton by the National Science Foundation and the Directorate of Chemical Sciences of the Air Force Office of Scientific Research.[15a]

---

(14) F. A. Gianturco and C. A. Coulson, *Mol. Phys.*, **14,** 223 (1968).

(15) F. A. Gianturco, "Influence of Chemical Substitution on Carbon 1s Electrons," Paper B1, Oxford University, Mathematical Institute, Wave Mechanics and Quantum Theory Progress Report, 1967–1968.

(15a) NOTE ADDED IN PROOF. Thomas[15b] has recently measured the binding energies of carbon 15 in the halomethanes. He finds smaller shifts for the fluoromethanes than those from the present wave functions (*e.g.*, 2.8 eV from CH_4 to CH_3F as compared to 4.85 eV from here) and attributes the discrepancy to the failure of the use of orbital energies to account for reorganization upon ionization. However, M. E. S.[15c] has recently completed calculations with more extended basis sets, and found that orbital energies do reflect energy shifts as well as those from direct calculation on both ground state and ion (*e.g.*, a shift of 3.2 eV from CH_4 to CH_3F is given by both methods with the extended basis). The discrepancy here is due[15c] to the inflexibility of the accurate *atomic* functions as *molecular basis* functions in accounting for inner-shell energies. Experimentally,[15b] the shifts are still linear and additive and the extended basis calculations[15c] do show the same sort of charge-dipole behavior found here; (b) T. D. Thomas, submitted for publication; (c) M. E. Schwartz, submitted for publication.

Translational Energy Dependence of the Bond Energy Effect for Abstraction from *n*-Perdeuteriobutane by Fast Hydrogen Atoms

Richard George Gann, Will Mann Ollison, and J. Dubrin

Contribution from the Department of Chemistry, Massachusetts Institute of Technology, Cambridge, Massachusetts 02139. *Received July 17, 1969*

Abstract: Hydrogen atoms at various well-known initial kinetic energies, 0.67, 0.92, 1.15, 1.67, and 2.05 eV, were generated by the photodissociation of HI and HBr and reacted with *n*-C_4D_{10} and *n*-$CD_3(CH_2)_2CD_3$. Abstraction at the weaker secondary C–D bonds is strongly favored over reaction at the primary positions (the bond energy effect was first observed in recoil systems, where the T is produced at essentially infinite energy on the chemical scale). The integrated yield ratio, HD(prim)/HD(sec), increases from 0.24 at the lowest source energy to 0.59 at the highest source energy. This significant energy dependence is consistent with a higher threshold energy for primary abstraction. At high relative energies (~2 eV), where the individual abstraction cross sections are only weakly energy dependent, the secondary cross section is ~30–50% greater than the primary cross section.

The familiar atomic hydrogen-saturated hydrocarbon abstraction reaction has been extensively investigated at thermal energies under equilibrium conditions,[1] very high kinetic energies in recoil media,[2] and at intermediate energies in photolytic systems.[3] Equilibrium thermal measurements can give little information about the energy-dependent form or size of the reaction cross section at energies much greater than the threshold energy. Indeed, $k(T)$ measurements of extremely high accuracy are necessary to distinguish the commonly used line of centers cross section form from other possible threshold excitation functions.

In the last 10 years two nonequilibrium techniques have been widely used to study H-saturate kinetics. In the recoil method, atomic tritium is produced at essentially infinite energy on the chemical scale and hence its chemistry may be conveniently observed over the whole reactive range (~50–0.5 eV). The fast tritiums undergo two major reaction modes with saturates.[2]

$$\begin{aligned} T + CH_4 &\longrightarrow TH + CH_3 \text{ (abstraction)} \\ &\longrightarrow CH_3T + H \text{ (displacement)} \end{aligned}$$

The abstraction threshold energy is ~0.3–0.5 eV, whereas, the rather unique displacement process has a threshold of 1.5–2.0 eV. A collision model for the displacement or exchange reaction has been discussed in detail by Wolfgang.[2]

---

(1) A. F. Trotman-Dickenson, "Gas Kinetics," Butterworth and Co., Ltd., London, 1955; V. N. Kondratev, "Chemical Kinetics of Gas Reactions," Addison Wesley Co., Reading, Mass., 1964; I. Amdur and G. G. Hammes, "Chemical Kinetics: Principles and Selected Topics," McGraw-Hill Book Co., Inc., New York, N. Y., 1966.

(2) R. Wolfgang, *Ann. Rev. Phys. Chem.*, **16,** 15 (1965); E. K. C. Lee and F. S. Rowland, *J. Amer. Chem. Soc.*, **85,** 897 (1963).

(3) (a) R. J. Carter, W. H. Hamill and R. R. Williams, Jr., *ibid.*, **77,** 6457 (1955); (b) R. M. Martin and J. E. Willard, *J. Chem. Phys.*, **40,** 3007 (1964).

In the photolytic technique, hydrogen atoms of different well-known initial kinetic energies (~0.3-4 eV) may be selectively generated by the photodissociation of a hydrogen halide in the presence of the reactant. Using this method, excitation function[4] and threshold energy measurements[5] have been made for a number of hydrogen atom reactions.

Extensive recoil investigations by Rowland and coworkers[6-10] have demonstrated the existence of a "bond energy effect"; the HT (DT) abstraction yield per CH (CD) bond decreases significantly with increasing bond dissociation energy. Rowland has explained this effect on the basis of an "energy cut off" model which correlates the yield behavior with the known lower activation energies for abstraction at weaker CH (CD) bonds. This model requires that the bulk of abstraction occurs at relatively low energies (<3 eV) where the integrated cross product of the collision density and reaction probability is postulated to increase with decreasing bond strength.[9]

Wolfgang[2,11-13] has proposed that the bulk of abstraction takes place at higher energies by a stripping mechanism which favors abstraction at the weaker bond. The latter hypothesis then predicts that the mean energy of abstraction increases with decreasing bond strength. The two bond energy models then differ chiefly in their estimates of the energy of the reacting tritium.

In order to see if a bond energy effect exists at initial relative kinetic energies of several electron volts, we have used the photolytic method and measured the HD abstraction yields for reactions 1 and 2 at five initial H energies: 0.67, 0.92, 1.15, 1.67, and 2.05 eV. The

$$\underset{\text{(secondary abstraction)}}{H + C_4D_{10} \longrightarrow HD + C_4D_9(\text{sec})} \tag{1}$$

$$\underset{\text{(primary abstraction)}}{H + C_4D_{10} \longrightarrow HD + C_4D_9(\text{prim})} \tag{2}$$

primary bond dissociation energy in butane is 0.14 ± 0.04 eV greater than the secondary dissociation energy. Since the steady state collision densities could be theoretically obtained, it was possible to correlate the observed yield differences between eq 1 and 2 with the corresponding differences in certain of the cross section parameters. This is the first bond energy study at intermediate energies (threshold – 2 eV) providing this type of information. However, for two reasons given in the Discussion, it is strongly felt that the present data are insufficient to decide whether the bulk of *recoil* abstraction occurs above or below a few electron volts.

General Approach

A brief description of the experimental techniques and theoretical analysis is given elsewhere.[4,14] Abstraction yields from the primary and secondary positions of butane were distinguished by separately reacting the fast hydrogens with n-C_4D_{10} and n-$C_4D_6H_4$-1,1,1,4,4,4-d_6. Secondary isotope effects on the yield ratios are assumed to be negligible. A comparison of the primary and secondary reaction cross sections can only be made properly if the collision densities corresponding to each initial source energy, $n'(E)$, $n''(E)$, etc., are known for both systems. Since little is known about either the magnitude or energy dependence of the various H-polyatomic inelastic (nonreactive) scattering cross sections at these high relative energies, the experimental yields were ultimately determined in butane systems diluted with a large excess of rare gas, Xe. By taking the appropriate limit of the yields (Appendix), the collision density solutions required only a knowledge of the H–Xe interatomic potential.

Experimental Section

Reagents. The C_4D_{10} and $C_4D_6H_4$ were obtained from Merck Sharp and Dohme of Canada, Ltd. The isotopic purity of the C_4D_{10} was approximately 98%; the minimum isotopic purity of the $C_4D_6H_4$ was 98.3%. The HI, HBr, and Xe were obtained from the Matheson Co., and prior to use air, H_2, and Br_2 or I_2 were removed. Hydrogen and HD for calibration purposes were obtained from the Matheson Co. and Mallinckrodt Nuclear, respectively.

Photolysis Cells. Irradiations at 2138, 2288, 3130, and 3340 Å were carried out in cylindrical quartz cells, 2.4-cm i.d. and 30-cm length. For the 2537-Å photolysis, cylindrical quartz cells, 2.1-cm i.d. and 15-cm length were employed. Each cell was equipped with a Fisher Porter Teflon stopcock and connected to the vacuum line by means of glass "O" ring joints.

Table I. Light Sources and Filters

E_L, eV[a]	Light source	Exciting photolysis "line," Å	Filtering system
0.67	200 W high P[f] Hg arc[b]	3340 (band)	Interference filter: 60 Å band pass (FWHM) + glass uv cut off filter
0.92	200 W high P Hg arc	3130 (band)	K_2CrO_4, KHPh solution filter + Pyrex uv cut off filters
1.15	25 W low P Hg arc[c]	2537	No. 7910 Vycor filter (removal of 1849 Å)
1.67	25 W low P Cd arc[d]	2288	Interference filter: 100 Å band pass (FWHM) (removal of 2144 Å)
2.05	25 W low P Zn arc[e]	2138	*cis*-Butene-2 gas filter: path length: 2 cm; pressure: 10 cm (removal of 2025, 2062 Å)

[a] HI was photolyzed for E_L = 0.67 and 0.92 eV and HBr was photolyzed for E_L = 1.15, 1.67, and 2.05 eV. [b] Osram, HBO-200W, supplied by Kenneth A. Dawson Co., Belmont, Mass. [c] Custom built by Hanovia Lamp Division of Engelhard Hanovia, Inc., Newark, N. J. [d] Phillips Arc, No. 93107E/CD, supplied by Ealing Corp., Cambridge, Mass. [e] Phillips Arc, No. 93106E/ZN, supplied by Ealing Corp., Cambridge, Mass. [f] P = pressure

Light Sources and Filters. The arcs and filter systems are described in Table I. The calculated average initial laboratory energy of the hydrogen corresponding to each photolysis wavelength is also listed there. The initial hydrogen atom energy was calculated from the following expression

$$E_L = \frac{m_X}{m_{HX}}[E_\lambda - D_0{}^\circ(HX) + \bar{E}_{rot}(HX)]$$

where m_X and m_{HX} are the masses of the halide and hydrogen ha-

---

(4) R. G. Gann and J. Dubrin, *J. Chem. Phys.*, **50**, 535 (1969).

(5) (a) C. C. Chou and F. S. Rowland, *ibid.*, **50**, 2763 (1969); (b) A. Kuppermann and J. M. White, *ibid.*, **44**, 4352 (1966).

(6) J. Root and F. S. Rowland, *J. Amer. Chem. Soc.*, **84**, 3027 (1962).

(7) W. Breckenridge, J. Root, and F. S. Rowland, *J. Chem. Phys.*, **39**, 2374 (1963).

(8) J. Root, W. Breckenridge, and F. S. Rowland, *ibid.*, **43**, 3694 (1965).

(9) E. Tachikawa and F. S. Rowland, *J. Amer. Chem. Soc.*, **90**, 4767 (1968).

(10) C. C. Chou, T. Smail, and F. S. Rowland, *ibid.*, **91**, 3104 (1969).

(11) D. Seewald and R. Wolfgang, *J. Chem. Phys.*, **47**, 143 (1967).

(12) R. T. K. Baker and R. Wolfgang, *J. Amer. Chem. Soc.*, **90**, 4473 (1968).

(13) R. T. K. Baker and R. Wolfgang, *J. Chem. Phys.*, in press.

(14) R. G. Gann and J. Dubrin, *ibid.*, **47**, 1867 (1967).

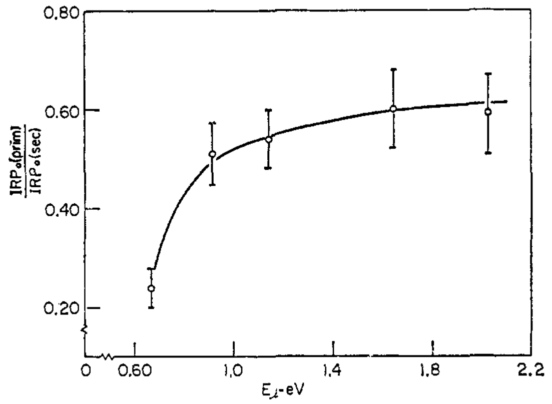

Figure 1. IRP_0(prim)/IRP_0(sec) *vs.* initial relative kinetic energy, E_i.

lide, E_λ is the photon energy, $\bar{E}_{\mathrm{rot}}(\mathrm{HX})$ is the average rotational energy of the HX, and $D_0°(\mathrm{HX})$ is the HX bond dissociation energy. The contribution to E_{L} from the HX thermal translational energy has been neglected in these calculations. (At room temperature this additional contribution to the hydrogen atom energy is on the average about 4×10^{-4} eV.) The initial relative kinetic energy is $^{68}/_{69}E_{\mathrm{L}}$ and $^{64}/_{65}E_{\mathrm{L}}$ for C_4D_{10} and $C_4D_6H_4$, respectively.

Procedure. The samples were filled on high-vacuum lines. Particular care was taken to avoid Hg contamination of the 2537-Å photolysis cells. Gaseous mixtures of various HX/butane composition ratios between 0.167 and 1.0 were filled and photolyzed. The HI samples were run at 273°K, whereas the HBr samples were irradiated at 295 ± 2°K. The per cent decomposition of the HX was maintained between 0.1 and 0.5%. The photolyzed samples were attached to a mass spectrometer sampling line, and after the butane and HX were solidified with liquid nitrogen, the relative quantities of H_2 and HD were measured with a quadrupole mass spectrometer. For a number of HX–butane mixtures dark experiments were carried out, and no H_2 or HD background signal was detectable.

Linear plots of the $[H_2]/[HD]$ product ratios *vs.* [HX]/[butane] composition ratios were found for all systems and their extrapolation to [HX]/[butane] = 0 yielded positive intercepts, I_0', I_0'', etc., in accord with the Carter, Hamill, Williams[15] equation.

$$\frac{[\mathrm{H_2}]}{[\mathrm{HD}]} = I_0' + \frac{k_3' + k_4'}{k_2'}\frac{[\mathrm{HX}]}{[\mathrm{butane}]} \qquad I_0' = \frac{k_1'}{k_2'}$$

The intercept is the ratio of the rate constants for moderation (k_1') by butane to hot reaction with butane (k_2'); k_3' and k_4' are similarly defined for HX (generally $k_4' \gg k_3'$). Neglecting the thermal motion of the medium, the fraction of hydrogens undergoing hot reaction between the initial source energy and the threshold is $(I_0' + 1)^{-1}$ in the absence of HX.

Although xenon is the poorest rare gas hydrogen atom moderator, it was chosen as the diluent to facilitate the product analysis. Since Xe has a very low vapor pressure at liquid nitrogen temperature, no prior gas chromatographic or other separation was required. (In the presence of a large pressure of a noncondensable gas, the product sampling rate has to be significantly reduced to maintain a sufficiently low vacuum for proper operation of the quadrupole analyzer. This gives rise to a relatively poor signal to noise ratio for the HD measurement.)

The $[H_2]/[HD]$ ratio was determined at various Xe dilutions corresponding to butane mole fractions, f, between 0.06 and 0.01. For *each* butane at each initial energy the HD yield $Y_0'(f)$, was determined

$$Y_0'(f) = ([\mathrm{H_2}]/[\mathrm{HD}] + 1)^{-1}$$

The ratio, $Y_0'(f)/f$, was plotted against f and extrapolated to $f = 0$ using a modified Carter, Hamill, Williams equation. These resulting intercepts will be referred to as "experimental limiting integral reaction probabilities," IRP_0'. Theoretical expressions for these integral probabilities in terms of the collision densities and excitation functions are derived in the Appendix.

Results

The integral reaction probability for secondary deuterium atom abstraction is obtained by difference (see Appendix): $IRP_0'(\mathrm{sec}) = IRP_0'(C_4D_{10}) - IRP_0'(C_4D_6H_4)$. In Table II, relative values of the IRP_0(prim) and IRP_0(sec) are listed as a function of initial relative kinetic energy.

Table II. Relative Integral Reaction Probabilities[a]

E_i, eV[b]	IRP_0 (sec)	IRP_0 (prim)	IRP_0(prim)/IRP_0(sec)
0.66	1.00	0.24	0.24 ± 0.04
0.91	1.83	0.93	0.51 ± 0.07
1.14	3.05	1.64	0.54 ± 0.06
1.64	4.02	2.40	0.60 ± 0.08
2.02	4.64	2.73	0.59 ± 0.08

[a] Measured IRP_0's are relative to IRP_0(sec) – 0.66 eV = 1.00. The absolute integral reaction probabilities may be obtained by multiplying the above by 0.50. [b] Initial relative energy.

The ratio IRP_0(prim)/IRP_0(sec) as a function of initial relative kinetic energy is shown in Figure 1. The analogous HD yield per CD bond is obtained by multiplying the ordinate by $^2/_3$.

Discussion

It is clear from Table II and Figure 1, that for *all* initial energies, attack at the secondary position is strongly favored over reaction at the primary position. On a normalized per C–D bond basis, the effect is even more pronounced; *e.g.*, at even the highest initial energy the secondary yield is greater than the primary yield by about a factor of 2.5. Regardless of the method of comparison, a large bond energy effect is operative over this intermediate energy range and is strongly energy sensitive below $E_i = 1$ eV.[16] It should be stressed that the IRP_0 values are integrated yields, and thus (at a particular E_i) the finding that $IRP_0(\mathrm{sec}) > IRP_0(\mathrm{prim})$ does not necessarily mean that $S_R(E)_{\mathrm{sec}} > S_R(E)_{\mathrm{prim}}$ for all E equal to or less than the initial relative energy (see below).

From a recent study[4] and the evaluation of the *IRP* integrals (see Appendix), it is known that the $S_R(E)_{\mathrm{sec}}$ has a threshold energy of about 0.30–0.35 eV and increases less than 20% in passing from E = 1–2 eV. For this latter reason and the finding from Figure 1 that IRP_0(prim)/IRP_0(sec) is relatively flatf rom 1 to 2 eV initial energy, it is reasonable to believe that the corresponding cross section ratio would increase only slightly over this large energy increment. We have quantitatively confirmed this expectation and found that the increase in the cross section ratio is between 5 and 15%. Furthermore, since the $dS_R(E)_{\mathrm{sec}}/dE$ and $dS_R(E)_{\mathrm{prim}}/dE$ are nearly zero for $E \cong 1.5$ eV, we can approximately equate the cross section ratio in this region to the asymptotic cross section ratio,[16,17] $S_R^0(E)_{\mathrm{prim}}/S_R^0(E)_{\mathrm{sec}}$.

---

(15) R. J. Carter, W. H. Hamill, and R. R. Williams, *J. Amer. Chem. Soc.*, 77, 6457 (1955).

(16) Although the IRP_0 ratios for $E_i > 1$ eV are energy independent within the errors cited, the bond energy effect as defined elsewhere[6,10] still exists for these initial energies, since the yield ratio is less than 1.5. The primary intent of this paper is to relate the differences in the integral reaction probability values to differences in the threshold energies and cross sections. The calculation of the cross section ratio at energies of several electron volts is not dependent on the particular "energy cut off" model that one wishes to interpret from the data of Table II.

(17) A more credible assignment of the energy region corresponding to the cross section maxima, must await the completion of experiments

The former cross section ratio is 0.65–0.75 and thus

$$S_R^0(E)_{\text{prim}}/S_R^0(E)_{\text{sec}} \cong 0.65\text{–}0.75$$

Though it is commonly known that the activation energy for abstraction (see below) increases with increasing bond strength, this is the first direct evidence that at high energies (∼2 eV) the cross section is a function of the bond energy. A mechanistic explanation for the significant difference in the reaction cross sections is presently unknown.

The sharp drop-off in the yield ratio below $E_i = 1$ eV is a result of either a large threshold energy increment or a significant difference in the shapes of the excitation functions. The two extreme models are then:

(A) E_0(prim) > E_0(sec), but both excitation functions have the same relative energy dependence above their respective threshold energies. $S_R(E)_{\text{sec}} = f(E, E_0(\text{sec}))$ and $S_R(E)_{\text{prim}} = Cf(E, E_0(\text{prim}))$, where C is a constant >1. The threshold energy increment, ΔE_0, is E_0(prim) − E_0(sec).

(B) E_0(prim) = E_0(sec), but with increasing energy above E_0, $S_R(E)_{\text{sec}}$ increases more rapidly than does $S_R(E)_{\text{prim}}$. For experimental reasons we have been unable as yet to determine E_0(prim). However, it is felt that case A is more important since it is known from extensive thermal H atom and CH_3 radical studies that there is a large difference in the activation energies for abstraction at the primary and secondary position of alkanes[18] (we are necessarily assuming that $\Delta E_a \cong \Delta E_0$), and preliminary calculations for a reasonable $\Delta E_0 = 0.1$ eV roughly simulate the abrupt yield behavior at low energies. For case B, $\Delta E_0 = 0$, a rather complex excitation function vastly different from the secondary form is required to fit the data.

The "energy cut off model" assumes that abstraction can occur down to lower energies for weaker C–H bonds due to the correspondingly lower threshold energy. The term "energy cut off" defined in this unrestricted manner can be misleading in that it suggests for $E_i \gg \Delta E_0$, the large yield differences arise from the added reaction between E_0(prim) and E_0(sec). For $E_i = 2$ eV and $\Delta E_0 = 0.1$ eV, only about 5% of the total secondary D yield results from reaction in this narrow energy band, which is considerably less than the 60–70% yield difference. Our direct evidence then confirms the recent conclusion of Tachikawa and Rowland[9] that yield differences in the vicinity of the threshold could not quantitatively account for the sizable bond energy effect. Instead, in a modification of the model, it was hypothesized that between threshold and about 3 eV, the reaction probability also exhibited a similar correlation with bond strength.[9] The combined effect of an *increasing* collision density and a *decreasing* cross section ratio, $S_R(E)_{\text{strong}}/S_R(E)_{\text{weak}}$, both with decreasing energy, could explain the large yield differences. For the system investigated here it is known that below 1 eV, $S_R(E)_{\text{prim}}$ falls off more rapidly with decreasing energy than $S_R(E)_{\text{sec}}$, and in passing from 2 eV to threshold, there is nearly a fivefold increase in the collision density. However, these factors are not of sole importance in determining the yield ratio for high initial energies (E_i = 1.5–2 eV); rather, the bond energy ratio largely reflects the sizable, *intrinsic* differences in the primary and secondary reaction cross sections at higher energies.[19] The finding that the yield ratio and the ratio of the asymptotic cross sections are not greatly different is not surprising, since both excitation functions rise rapidly with increasing energy above their respective thresholds. At relatively high initial energies then, the net effect of the higher collision density at lower energies is nearly "washed out." It should be emphasized that unless the yield measurements are carried out at a number of initial energies and in media where the collision density can be theoretically calculated, it is exceedingly difficult to interpret these ratios in terms of differences in the cross section parameters.[9]

Other Photolytic Studies. Martin and Willard[3b] have measured HD yields from the reaction of 2.8-eV H with CD_4, C_2D_6, and D_2, and the isotopically reversed system 2.8-eV D with CH_4, C_2H_6 and H_2. Since the determinations were carried out in media of different, unknown moderating power and at only one initial energy, a number of assumptions were necessary to extract average reaction probabilities, $\bar{p}(E)$. It was found, though, that $\bar{p}(E)_{\text{ethane}} > \bar{p}(E)_{\text{methane}}$ ($D_0°$(methane) − $D_0°$(ethane) ≅ 0.16 eV), consistent with our findings.

Chou and Rowland have very recently reported[10] relative abstraction yields from reaction of photolytically generated 2.8-eV T with a number of deuterated hydrocarbons. The relative DT yields increased with decreasing bond strength and in general were about the same size as the correponding (relative) recoil yields. On the basis of this agreement and the approximate similarity between the *absolute* photolytic and recoil abstraction yields, it was inferred that a sizable part of the observed recoil yield results from low energy reactions.

Photolytic and Recoil Yield Comparisons. The comparison of photolytic with recoil bond energy determinations is not a very rigorous means of deciding whether the bulk of abstraction in recoil *hydrocarbon systems* occurs in the few eV range or at much higher energies. To measure the ratios, a large excess of either a rare gas or, more commonly, a reactive polyatomic is added to the systems to provide a uniform collision environment. In doing this, though, the original systems are disturbed; and, depending on the choice of additive, the deduction of the average abstraction energy on the basis of the agreement of the yield ratios may be ambiguous. The finding that absolute yields and bond energy ratios are similar for both the recoil and photolytic systems should only be considered as consistent evidence for the low energy hypothesis. In addition, for our system, it is unknown what effect substitution of H for T has on the cross section ratio, $S_R(E)_{\text{strong bond}}/S_R(E)_{\text{weak bond}}$, and thus the yield ratio. For these two reasons, we feel it is not meaningful to contrast our results with recoil measurements.

The original question can possibly be answered without resorting to photolytic measurements, but instead determining the yields in rare gas recoil media. Assuming that the hot atom kinetic theory in its present form provides meaningful reaction energy estimates, the average energy of displacement and abstraction can be

---

at higher E_i. (A definite decrease in the $S_R(E)$ must be observable to locate the energy maximum.) The cross section derivatives are extremely sensitive to the exact shape of the experimental, integral reaction probability curve.

(18) A. F. Trotman-Dickenson, *Advan. Free-Radical Chem.*, 1, 1 (1965).

(19) Tachikawa and Rowland give various cross section–collision density plots to clarify the "energy cut off" model (ref 9). Our findings are in general agreement with case 2 (middle and lower diagrams of Figure 2).

related.[11-13] Since there is actually agreement that almost all displacement occurs at energies in excess of 3 eV, a finding that $\bar{E}$(abstraction) > $\bar{E}$(displacement) would indicate that the bulk of recoil abstraction occurs at $E > 3$ eV. Subsequent competitive rare gas experiments are useful in determining the $\bar{E}$(abstraction) as a function of bond strength.[12]

Future Studies. Future rare gas photolytic and recoil experiments together with atomic T beam measurements will provide detailed information about the abstraction excitation function over the whole reactive range. Conclusive proof of the reaction mechanism will be realized through the measurement of the angular and velocity distributions of the scattered product. Thus, as in the case of ion-molecule reactions,[20] one will be able to answer the most interesting question: How does the "abstraction" mechanism change with relative kinetic energy?

Appendix: Rare Gas Collision Density Formulation

For a three-component system HX, Xe, and C_4D_{10}-(RD) the following definitions are given:

f, g—Mole fractions of RD and Xe, respectively. The mole fraction ratio, [RD]/[HX] is maintained constant for each initial energy.

$n'(E)_{RD}dE$—Steady state number of collisions a hydrogen atom makes with RD between E and $E + dE$ (relative energy) in a mixture with HX and Xe.

$n'(E_L)_{RD}dE_L$; $n'(E_L)_{Xe}dE_L$—Same as above, but in laboratory frame for RD and Xe.

$S_R(E)_{prim}$; $S_R(E)_{sec}$—Primary and secondary reaction cross sections.

$S(E)_{RD}$; $S(E)_{Xe}$—Total H atom scattering cross sections.

$S(E_L)_{RD}$; $S(E_L)_{Xe}$—Average total scattering cross sections for a hydrogen atom of laboratory energy, E_L.

$G(E, E_L)$—Normalized distribution function of relative kinetic energies between an atom of E_L and a target gas having a Maxwellian velocity distribution

$$G(E,E_L)dE = \frac{1}{2\mu}\left(\frac{m_1m_2}{\pi kTE_L}\right)^{1/2} \times \left(\exp\left\{-\frac{m_2}{2kT}\left[\left(\frac{2E_L}{m_1}\right)^{1/2} - \left(\frac{2E}{\mu}\right)^{1/2}\right]^2\right\} - \exp\left\{-\frac{m_2}{2kT}\left[\left(\frac{2E_L}{m_1}\right)^{1/2} + \left(\frac{2E}{\mu}\right)^{1/2}\right]^2\right\}\right) dE$$

where m_1 is the mass of the the atomic hydrogen; m_2 is the mass of either RD or Xe; μ is the reduced mass; T is the temperature of the target mixture.

Employing the Miller-Dodson formula,[21] the fractional HD yield may be related to the collision density and reaction probability, $p(E) = S_R(E)/S(E)$, by

$$\frac{[HD]}{[H_2 + HD]} = Y_0'(f) = \int_{E_0(sec)}^{\infty} n'(E)_{RD}\frac{S_R(E)_{sec}}{S(E)}\,dE + \int_{E_0(prim)}^{\infty} n'(E)_{RD}\frac{S_R(E)_{prim}}{S(E)}\,dE \quad (1)$$

$$n'(E_L)_{RD}dE_L = n'(E_L)_{Xe}\left(\frac{f}{g}\right)\frac{S(E_L)_{RD}}{S(E_L)_{Xe}}\,dE_L \quad (2)^{22}$$

$$n'(E)_{RD}dE = \left[\int_0^{\infty} n'(E_L)_{Xe}G(E_L, E)dE_L\right]dE \quad (3)$$

where $m_2 = m(C_4D_{10})$.

Expressing (3) in terms of (2) and inserting into (1)

$$Y_0'(f) = \int_{E_0(sec)}^{\infty} \frac{S_R(E)_{sec}}{S(E)_{RD}}\int_0^{\infty} n'(E_L)_{Xe}\left(\frac{f}{g}\right)\frac{S(E_L)_{RD}}{S(E_L)_{Xe}} \times G(E_L, E)dE_L\,dE + \text{primary integral} \quad (4)$$

Dividing by f and taking the limit as $f \rightarrow 0$

$$\lim_{f\to 0}\frac{Y_0'(f)}{f} = IRP_0'(C_4D_{10}) = \int_0^{\infty}\frac{S_R(E)_{sec}}{S(E)_{RD}}\int_0^{\infty} n_0'(E_L)_{Xe}\frac{S(E_L)_{RD}}{S(E_L)_{Xe}} \times G(E_L, E)dE_L\,dE + \text{primary integral} \quad (5)$$

where $n_0'(E_L)_{Xe}$ is the collision density for atomic hydrogen in a pure, Xe medium.

Since $S(E_L) = \int_0^{\infty} S(E)G(E, E_L)\,dE$, $m_2(RD) \gg m_1(H)$, and $E_L \gg kT$, with negligible error eq 5 may be simplified.

$$IRP_0'(C_4D_{10}) = \int_{E_0(sec)}^{\infty} S_R(E)_{sec}\int_0^{\infty}\frac{n'_0(E_L)_{Xe}}{S(E_L)_{Xe}}\,G(E_L, E)dE_L dE + \int_{E_0(prim)}^{\infty} S_R(E)_{prim}\int_0^{\infty}\frac{n_0'(E_L)_{Xe}}{S(E_L)_{Xe}}\,G(E_L, E)\,dE_L dE$$

Similarly for $C_4D_6H_4$ (primary abstraction only)

$$\lim_{f\to 0}\frac{Y_0'(f)}{f} = IRP_0'(C_4D_6H_4(prim)) = \int_{E_0(prim)}^{\infty} S_R(E)_{prim}\int_0^{\infty}\frac{n_0'(E_L)_{Xe}}{S(E_L)_{Xe}}\,G(E_L, E)\,dE_L dE \quad (7)$$

where now $m_2 = m(C_4D_6H_4)$.

Again, since $m_2 \gg m_1$ and $m_2(C_4D_6H_4) \cong m_2(C_4D_{10})$, with little error eq 6 and 7 are combined

$$IRP_0'(sec) = IRP_0'(C_4D_{10}) - IRP_0'(C_4D_6H_4(prim)) \quad (8)$$

The H-Xe collision density is calculated stochastically.[23] For the purposes of this study a modified Buckingham potential ($\alpha = 10$, $r_m = 4$ Å, and $\epsilon = 0.025$ eV) was employed to represent the H-Xe interaction.

---

(20) W. R. Gentry, E. A. Gislason, Y. Lee, B. H. Mahan, and C. Tsao, *Discussions Faraday Soc.*, **44**, 137 (1967); Z. Hermann, J. Kerstetter, T. Rose, and R. Wolfgang, *Discussions Faraday Soc.*, **44**, 123 (1967).

(21) J. M. Miller and R. W. Dodson, *J. Chem. Phys.*, **18**, 865 (1950).

(22) The neglect of the relative velocity dependence upon mass is an excellent approximation here (the error is less than 0.1%). These and other approximations will be critically discussed elsewhere.[23]

(23) C. Rebick and J. Dubrin, submitted for publication.